

Inhibition of oxidative stress by apocynin attenuated COPD progression and vascular injury by cigarette smoke exposure

Stanley Chan¹, Kurt Brassington², Suleman Almerdasi¹, Aleksandar Dobric¹, Simone De Luca¹, Madison Coward-Smith¹, Hao Wang¹, Kevin Mou¹, Alina Akhtar¹, Rana Alateeq¹, Wei Wang¹, Huei Seow¹, Stavros Selemidis¹, Steven Bozinovski¹, and Ross Vlahos¹

¹RMIT University

²RMIT University College of Science Engineering and Health

December 14, 2022

Abstract

Background and Purpose: Cardiovascular disease (CVD) affects up to half of the patients with chronic obstructive pulmonary disease (COPD), which exerts deleterious impact on health outcomes and survivability. Vascular endothelial dysfunction marks the onset of cardiovascular disease. The present study examined the effect of a potent NADPH Oxidase (NOX) inhibitor and free-radical scavenger, apocynin, on COPD-related CVD. **Experimental Approach:** Male BALB/c mice were exposed to either room air (Sham) or cigarette smoke (CS) generated from 9 cigarettes per day, 5 days a week for up to 24 weeks with or without apocynin treatment (5 mg·kg⁻¹·day⁻¹, intraperitoneal injection). **Key Results:** Eight-weeks of apocynin treatment reduced airway neutrophil infiltration (by 42%) and completely preserved endothelial function and endothelial nitric oxide synthase (eNOS) activity against the oxidative insults of CS exposure. These preservative effects were maintained up until the 24-week time point. 24-week of apocynin treatment exhibited marked benefits on airway inflammation (reduced infiltration of macrophage, neutrophil and lymphocyte) and lung function decline (hyperinflation), and prevented airway collagen deposition by CS exposure. **Conclusion and Implications:** Limiting NOX activity may slow COPD progression and lower CVD risk, particularly when signs of oxidative stress become evident.

Inhibition of oxidative stress by apocynin attenuated COPD progression and vascular injury by cigarette smoke exposure

Stanley MH Chan, Kurt Brassington, Suleman Abdullah Almerdasi, Aleksandar Dobric, Simone N De Luca, Madison Coward-Smith, Hao Wang, Kevin Mou, Alina Akhtar, Rana Abdullah Alateeq, Wei Wang, Huei Jiunn Seow, Stavros Selemidis, Steven Bozinovski, Ross Vlahos*

School of Health and Biomedical Sciences, RMIT University, BUNDOORA,
VIC 3083, Australia

Running title: Apocynin attenuates smoking-induced COPD

***Author for correspondence**

Professor Ross Vlahos, PhD
School of Health and Biomedical Sciences
RMIT University, PO Box 71, Bundoora, VIC 3083 Australia
Tel: +61 3 9925 7362
Email: ross.vlahos@rmit.edu.au

Data availability statement: The data that support the findings of this study are available from the corresponding author upon reasonable request. Some data may not be made available because of privacy or ethical restrictions.

Funding statement: The authors would like to thank the National Health and Medical Research Council of Australia (Project Grant Numbers APP1084627 and APP1138915) for funding this work.

Author contribution statement: Concept and design: R.V., K.B., S.M.H.C.; acquisition of data: S.A., K.B., A.D., S.N.D., H.W., S.M.H.C., H.J.S; data analysis and interpretation: S.A., K.B., S.N.D., H.J.S., H.W., S.M.H.C., S.S., S.B., R.V.; technical assistance: A.D., M.C.S., K.M., A.A., R.A., W.W.; drafting, editing, and/or critical revision of the manuscript for intellectual content: all authors; R.V. provided the resources for the work to be performed and is the senior investigator ensuring accuracy and integrity of the work.

Conflict of interest statement:

The authors declare no conflict of interest in this study.

Word count: 3454

What is already known:

- Irreversible airflow limitation in COPD is due to narrowing and fibrosis of small airways.
- Cardiovascular disease (CVD) is a major COPD comorbidity that predicts disease morbidity and mortality.

What this study adds:

- Inhibition of oxidative stress lessens airflow limitation and airway fibrosis in a mouse model of COPD.
- Targeting oxidative stress also prevents the onset of endothelial dysfunction and platelet activation in COPD.

Clinical significance:

- Oxidative stress may be a useful “treatable trait” for the management of respiratory symptoms and CVD in COPD.

Abstract

Background and Purpose: Cardiovascular disease (CVD) affects up to half of the patients with chronic obstructive pulmonary disease (COPD), and exerts deleterious impact on health outcomes and survivability. Vascular endothelial dysfunction marks the onset of cardiovascular disease. The present study examined the effect of a potent NADPH Oxidase (NOX) inhibitor and free-radical scavenger, apocynin, on COPD-related CVD.

Experimental Approach: Male BALB/c mice were exposed to either room air (Sham) or cigarette smoke (CS) generated from 9 cigarettes per day, 5 days a week for up to 24 weeks with or without apocynin treatment ($5 \text{ mg} \cdot \text{kg}^{-1} \cdot \text{day}^{-1}$, intraperitoneal injection).

Key Results: Eight-weeks of apocynin treatment reduced airway neutrophil infiltration (by 42%) and completely preserved endothelial function and endothelial nitric oxide synthase (eNOS) availability against the oxidative insults of CS exposure. These preservative effects were maintained up until the 24-week time point. 24-week of apocynin treatment markedly reduced airway inflammation (reduced infiltration of macrophage, neutrophil and lymphocyte) and lung function decline (hyperinflation), and prevented airway collagen deposition by CS exposure.

Conclusion and Implications: Limiting NOX activity may slow COPD progression and lower CVD risk, particularly when signs of oxidative stress become evident.

Acknowledgements: The authors would like to thank the National Health and Medical Research Council of Australia (Project Grant Numbers APP1084627, APP1120522 APP1138915) for funding this work.

Keywords: Chronic inflammation, NADPH oxidase, treatable traits, hyperinflation, endothelial dysfunction, platelet activation

Abbreviations: AB-PAS, alcian blue-periodic acid Schiff; ARRIVE, animal research: reporting of in vivo experiments; ANOVA, analysis of variance; ATP, adenosine triphosphate; AUC, area under curve; BALF, bronchoalveolar lavage fluid; Ccl, Chemokine (C-C motif) ligand; COPD, chronic obstructive pulmonary disease; CRP, C-reactive protein; CS, cigarette smoking; CVD, cardiovascular disease; Cxcl2, Chemokine (C-X-C motif) ligand; DAPI, 4',6-diamidino-2-phenylindole; DMSO, dimethyl sulfoxide; EC₅₀, effective concentration at 50% of maximal relaxation; ELISA, enzyme-linked immunosorbent assay; eNOS, endothelial nitric oxide synthase; EPI, epididymal fat depot; FVC, forced vital capacity; Gastroc, gastrocnemius; H₂O₂, hydrogen peroxide; H&E, haematoxylin and eosin; IC, inspiratory capacity; Inter, interscapular fat depot; i.p., intraperitoneal; IL, interleukin; Mmp, matrix metalloproteinase; NFκB, nuclear factor kappa B; NO, nitric oxide; NOX, nicotinamide adenine dinucleotide phosphate oxidase; PBS, phosphate-buffered saline; PBST, phosphate-buffered saline with tween 20; PV, pressure-volume; Quads, quadriceps muscle; Retro, retroperitoneal fat depot; R_{max}, maximal relaxation response; ROS, reactive oxygen species; SEM, standard error of mean; Sol, soleus muscle; SNP, sodium nitroprusside; STATs, signal transducers and activators of transcription; TA, tibialis anterior muscle; TGF, transforming growth factor; TNF, tumor necrosis factor;

Introduction

Chronic obstructive pulmonary disease (COPD) is an inflammatory respiratory disease characterised by chronic airway obstruction and remodelling, and the destruction of lung tissues that interfere with normal breathing (WHO, 2022). The airway pathologies of COPD are largely irreversible, making COPD a major public health issue, affecting approximately 12% of individuals worldwide and incurring a substantial socioeconomic burden (Adeloye et al., 2015). While in industrialised countries, cigarette smoke (CS) exposure is the primary risk factor for the development of COPD, however, COPD may also be caused by combustion of biomass and air pollution in low- to middle-income countries (Safiri et al., 2022). In addition to pulmonary pathologies, COPD is associated with many comorbidities, such as cardiovascular disease (CVD), metabolic disorders, neurocognitive impairments, and musculoskeletal disorders, that further increase the probability of hospital admission and mortality, and thus reducing quality of life. In particular, CVD has been demonstrated to be a leading contributor to the morbidity and mortality of COPD and can be detected independently of traditional risk factors in approximately a third of COPD patients, accounting for about 50% of deaths (Rabe et al., 2018), even after adjustment for confounding factors (Balbirsingh et al., 2022). The increased morbidity and mortality could be attributed to, at least in part, more frequent exacerbations (Balbirsingh et al., 2022; Rabe et al., 2018). The observation that both CVD comorbidities and COPD have shared risk factors such as history of cigarette smoking or exposure to noxious gas/particles, accelerated ageing and physical inactivity (Brassington et al., 2019), and that the degree of airflow obstruction may be an independent predictor of adverse cardiovascular outcomes (Sin et al., 2005) are suggestive of a causal relationship between airflow limitation and CVD comorbidities in COPD (Sin et al., 2005). As both COPD and CVD comorbidities represent a significant global impact on health, understanding the pathophysiology between them could potentially reduce this burden (Balbirsingh et al., 2022).

Although yet to be fully established, the “spill-over” of local lung inflammation in COPD has been demonstrated to drive CVD risk (Barnes, 2019). In a preclinical model of COPD, Brassington *et al.* (Brassington et al., 2021) demonstrated that oxidative stress from CS exposure may cause inflammatory cell infiltration into the vascular wall and endothelial dysfunction, suggesting oxidative stress may be a missing link. In addition to marking the imbalance between reactive oxygen species (ROS) and endogenous antioxidant defence, oxidative stress may simultaneously exacerbate comorbidities, stimulating fibrosis and emphysema development of the lungs by amplifying chronic inflammation (Barnes, 2020). The vascular endothelium is a single layer that lines the interior surface of the vessels, responsible for the regulation of vasomotor tone, vascular permeability, coagulation cascade, angiogenesis and innate and adaptive immunity (Brassington et al., 2019). Endothelial dysfunction is the earliest stage of CVD comorbidities, characterised by an imbalance between endothelium-derived vasodilating (i.e. nitric oxide [NO], prostacyclin and endothelium-derived hyperpolarizing factor) and vasoconstricting factors (i.e. endothelin-1 and thromboxane) (Theodorakopoulou et al., 2021). In COPD, endothelial dysfunction may also be caused by the reduced bioavailability of NO from the inflammatory-mediated changes of the vascular walls, such as degradation and replacement of the elastic fibres that controls vascular tone and function by collagen, increasing arterial stiffness thus driving vascular dysfunction (Theodorakopoulou et al., 2021). Furthermore, persisting inflammation in COPD may also stimulate platelet activation, thereby establishing a pro-coagulant environment in the vasculature (Hlapcic et al., 2020). Together, endothelial dysfunction and a pro-coagulant

environment promote arterial remodelling that may lead to pulmonary hypertension, a condition that worsens gas exchange and dyspnoea, as well as vulnerability to right ventricular dysfunction (Hlapcic et al., 2020). Therefore, addressing endothelial dysfunction is expected to reduce CVD risk in COPD.

In the vasculature, NADPH oxidases (NOX) are considered the predominant sources of ROS that interferes with endothelial function (Brassington et al., 2019). Apocynin is a methoxy-substituted catechol derived from the herb *Picrorhiza kurroa* exhibiting NOX inhibitory properties by blocking the assembly of a functional NOX complex and/or via radical scavenging action, depending on its concentration (Petronio et al., 2013). At a dosage of 5 mg·kg⁻¹·day⁻¹, we have previously demonstrated that apocynin exerted good anti-inflammatory action and inhibitory effects on NOX2 (Oostwoud et al., 2016; Vlahos et al., 2011). Moreover, at this dosage, apocynin was able to prevent the loss of leg muscle mass and contractile function by CS exposure (Chan et al., 2021), suggesting inhibition of oxidative stress and inflammation may lower CVD risk in COPD. On this note, apocynin has been shown to restore endothelial function in streptozotocin-induced diabetic rats (Olukman et al., 2010). However, its effectiveness against COPD-related vascular impairment remains undetermined. In the present study, we aimed to define the effect of apocynin administration on the progression of COPD and vascular endothelial function following CS exposure.

Material and methods

Mice

Male BALB/c mice (7 weeks of age) were obtained from the Animal Resources Centre (Perth, WA, Australia). Mice were housed in micro-isolator cages at $21 \pm 0.5^\circ\text{C}$ on a 12-hour day/night cycle with *ad libitum* access to standard mouse chow diet and water. After 1 week of acclimatization, mice were randomly assigned to room air (Sham) or CS exposure groups, with or without daily supplementation of apocynin at $5 \text{ mg}\cdot\text{kg}^{-1}$ via intraperitoneal (i.p.) injection, $n=16$ per group. Apocynin was prepared daily by dissolving in DMSO, before further dilution in sterile saline to reach a final concentration of $\sim 0.05\%$ DMSO. The vehicle groups were injected with saline (containing $\sim 0.05\%$ DMSO). Mice of the respective cages were weighed three times a week with daily monitoring. All experiments were conducted in accordance with the Australian Code of Practice for the Care of Experimental Animals, the ARRIVE Guidelines and with RMIT University Animal Ethics Committee approval (Animal Ethics Application Number 1928).

Cigarette smoke exposure

Mice were placed in 18L perspex chambers and exposed to CS from three cigarettes (Winfield Red, 16 mg or less of tar, 15 mg or less of carbon monoxide, 1.2 mg or less of nicotine; Philip Morris, Australia) spaced evenly over 1 hour and carried out three times per day (09:00, 12:00, and 15:00 h), five days a week (Monday to Friday) for up to 24 weeks. The Sham mice were handled identically and exposed to room air. We have previously shown that this CS exposure protocol in male BALB/c mice recapitulates key clinical traits of human COPD, including lung inflammation and pathology (airway inflammation, emphysema and impaired lung function), increased lung and systemic oxidative stress and comorbidities including skeletal muscle dysfunction (Chan et al., 2020; Dobric et al., 2022). Hence, only male mice were included in the present study.

Body composition scan and blood analysis

Fat and lean contents were determined using an EchoMRI apparatus (Echo Medical Systems, Houston, TX, USA). To understand the systemic impact of CS exposure and apocynin treatment, whole blood was collected from the inferior vena cava at the end of the experiment and counted using a CELL-DYN Emerald hematology analyser (Abbott Core Laboratory, USA), as previously described (Dobric et al., 2022).

Lung function assessment, bronchoalveolar lavage and tissue collection

Mice were anaesthetised by i.p. injection with ketamine ($125 \text{ mg}\cdot\text{kg}^{-1}$) and xylazine ($25 \text{ mg}\cdot\text{kg}^{-1}$) and tracheotomy was performed by inserting an 18G canular into the trachea. Lung function of anaesthetised mice was measured using a flexiVent ventilator (Scireq Inc. Montreal, Canada) which employs different scripts including force oscillation, deep inflation and constant phase models in mice with a breathing rate of 150 breaths per minute. Deflation of the lungs were performed to generate inspiratory capacity (IC). Pressure-volume (PV) loops and negative pressure-driven forced expiratory (NPFE) were performed to obtain inspiratory capacity (IC), static compliance, forced vital capacity (FVC), the PV curve and the area enclosed by the PV loop area as previously performed (Dobric et al., 2022). Following lung function testing, mice were humanely killed by overdosing with sodium pentobarbitone ($240 \text{ mg}\cdot\text{kg}^{-1}$; Virbac, NSW, Australia) via i.p. injection.

Lungs were lavaged *in situ* using 0.4mL of ice-cold PBS and three subsequent repeats of 0.3mL PBS, with a return of approximately 1mL of bronchoalveolar lavage fluid (BALF) per mouse

as previously published (Chan et al., 2021; Chan et al., 2020). BALF (20 μ L) was diluted 1:1 with Acridine Orange and the total number of viable cells counted on a standard Neubauer haemocytometer under fluorescent light on an Olympus BX53 microscope (Olympus Corporation, Tokyo, Japan). To differentiate cell populations in BALF, cytocentrifuge preparations (Shandon Cytospin 3, 400 rpm, 10 min) were performed using $\sim 5 \times 10^4$ cells from the BALF. Once dried, cells were fixed with Shandon™ Kwik-Diff™ fixative (ThermoFisher Scientific, NY, USA) and subsequently stained with Hemacolor® Rapid Red and Blue dye (Merck, Darmstadt, Germany) as per manufacturers' instructions, mounted with Entellan® New (Merck, Darmstadt, Germany). Cell types (macrophages, lymphocytes, and neutrophils) were identified according to standard morphological criteria and at least 500 cells per slide were counted. After the lavage procedure, 10mL of PBS was used to clear the lungs of blood via a right ventricular perfusion of the heart. Lung tissues were then collected, snap frozen in liquid nitrogen and stored at -80°C until required.

Vascular myography

Vascular myography was used to assess vascular function as previously described (Brassington et al., 2021). Briefly, thoracic aortae were excised from the chest cavity, placed in a petri dish filled with carbogen-bubbled (95% O₂, 5% CO₂) Krebs buffer (NaCl 119, KCl 4.7, MgSO₄ 1.17, NaHCO₃ 25, KH₂PO₄ 1.18, CaCl₂ 2.5, glucose 5.5, all in mmol/L), before perivascular fat and connective tissue were carefully dissected away. The aortae were then cut into 2 mm rings and subject to vessel myography (*ex-vivo* functional testing) using a 4 channel myograph unit (Model 610M, Danish Myo Technology (DMT) A/S, Denmark).

Histology and immunostaining

In a separate cohort of mice, the excised aortae were fixed in 10% Neutral Buffer Formalin (Sigma-Aldrich, MO, USA) overnight at 4°C before subjecting to the Leica Tissue Processor (model ASP300, Leica Biosystems, MA, USA). The tissues were paraffin embedded using HistoCore Arcadia (Leica Biosystems, MA, USA), serial cross sections were cut using a microtome (Leica Biosystems, MA, USA) at 4 micron thickness onto Superfrost® Plus microscope slides (ThermoFisher Scientific, NY, USA). The sections were dewaxed and rehydrated as previously described (Brassington et al., 2022; Brassington et al., 2021), before antigen retrieval in sodium citrate buffer (10mM Sodium Citrate, 0.05% Tween 20 at pH 6.0), blocking and permeabilization (PBS containing 1% bovine serum albumin, 22.52 mg/mL glycine and 0.25% Triton X-100) as described on <https://www.abcam.com/protocols/immunocytochemistry-immunofluorescence-protocol>.

For lung histology, haematoxylin and eosin (H&E) and Alcian blue-periodic acid Schiff (AB-PAS) and Masson's trichrome stains were processed at Melbourne Histology Platform (University of Melbourne, Melbourne, VIC, Australia) were performed for the assessment of tissue inflammation, airway mucus and airway collagen as previously described (Wang et al., 2021).

For aortic immunostaining, specific primary antibodies were used to detect vascular endothelial nitric oxide synthase (eNOS; anti-NOS3 at 1:100 dilution; Thermo Fisher Scientific, USA), vascular peroxynitrite (anti-3-Nitrotyrosine [3-NT] at 1:100 dilution; ThermoFisher Scientific, NY, USA), platelet surface marker Integrin alpha 2b (anti-CD41 at 1:100 dilution; Bioss Antibodies, MA, USA), platelet activation marker p-selectin (anti-CD62p at 1:100 dilution; Bioss Antibodies, MA, USA). After an overnight incubation at 4°C, the sections were washed before exposure to fluorescent-conjugated secondary antibody (Goat anti-Rabbit IgG Fluor™

488; ThermoFisher Scientific, NY, USA) for 2 h at room temperature, light protected. After washing, the sections were coverslipped using Fluoromount-G™ mounting medium containing DAPI (ThermoFisher Scientific, NY, USA) and imaged on an Olympus Slide Scanner (VS120-S5, Olympus Corporation, Tokyo, Japan), and analysed using Olympus cellSens Dimension™ desktop software (version 1:18, Olympus Corporation, Tokyo, Japan). Positive signals (n= 8 per group) are expressed as fluorescence intensity fold change or area of positive stain as previously described (Brassington et al., 2022; Brassington et al., 2021; Chan et al., 2021; Chan et al., 2020). All analysis was completed in a blinded manner, conforming with BJP guidelines (Alexander et al., 2018).

Gene expression analysis

Total RNA was extracted from frozen lung tissue with a RNeasy Mini kit (Qiagen, MD, USA). cDNA was prepared with a High Capacity RNA-to-cDNA Kit (ThermoFisher Scientific, NY, USA). qPCR was performed using pre-developed TaqMan™ gene expression assays (**Table 1**; ThermoFisher Scientific, NY, USA). The threshold cycle values (Ct) were normalised to a reference gene (glyceraldehyde phosphate dehydrogenase; GAPDH) and the relative fold change was determined by the $\Delta\Delta C_t$ method (Chan et al., 2021; Vlahos et al., 2011).

Table 1. List of gene expression assays

Gene name	Abbreviation	Taqman assay ID
Chemokine (C-C motif) ligand 2	<i>Ccl2</i>	Mm00441242_m1
Chemokine (C-X-C motif) ligand 2	<i>Cxcl2</i>	Mm00436450_m1
Cytochrome b-245, beta polypeptide (NADPH oxidase 2)	<i>Cybb</i>	Mm01287743_m1
Interleukin-6	<i>Il6</i>	Mm00446190_m1
Tumour necrosis factor	<i>Tnfa</i>	Mm00443258_m1
Matrix metalloproteinase 12	<i>Mmp12</i>	Mm00500554_m1
NADPH oxidase 4	<i>Nox4</i>	Mm00479246_m1

Data and Statistical Analysis

All data and statistical analysis comply with the recommendations on experimental design and analysis in pharmacology (Curtis et al., 2018). Data are presented as mean + standard errors of the mean (SEM). Statistical differences between treatments were determined by 2-tailed unpaired t-test or analysis of variance (ANOVA) followed by Tukeys multiple comparison post-hoc tests where appropriate. One-way ANOVA were used for three or more unmatched groups. Two-way ANOVA were used to analyse data when response was influenced by two independent factors of interest. All statistical analyses were performed using GraphPad Prism for Microsoft Windows® (Versions 9, Graphpad software®, CA, USA) where $p < 0.05$ was accepted as significant for all cases.

Results

Apocynin treatment attenuated the deterioration in vascular endothelial function, vascular oxidative stress and injury by CS exposure.

Similar to our previous observations (Brassington et al., 2021; Chan et al., 2021), eight weeks of CS exposure resulted in marked airway inflammation evidenced by the 4.6-fold increase in total number of cells present in the BALF (**Figure S1A**), which are predominantly composed of macrophages and neutrophils, and lymphocytes (**Figure S1B-D**) to a minor extent. In line with the BALF cell count, CS exposure increased the expression of key pro-inflammatory mediators: *Tnfa*, *Il6* and *Mmp12* (**Figure S1E-G**) and chemoattractants: *Ccl2* and *Cxcl2* (**Figure S1H and I**). CS exposure also increased the expression of *Cybb* (encodes for NOX2, **Figure S1J**) in the lungs, but not *Nox4* (**Figure S1K**), indicating a NOX2-dependent nature of this CS-induced airway inflammation. Despite a 42% reduction in BALF neutrophil count (**Figure S1C**), apocynin treatment had no significant effects on the expression of pro-inflammatory mediators, chemoattractants or *Cybb* by CS exposure (**Figure S1E-K**), suggesting the overall inflammatory status remained unchanged at this early time point.

To assess the effects of apocynin treatment on vascular function, precontracted thoracic aorta segments were exposed to increasing concentrations of acetylcholine to examine endothelial-dependent relaxation responses. CS exposure significantly impaired aortic vasodilation to acetylcholine, evidenced by the altered acetylcholine relaxation curve and an increased EC₅₀ (**Figure 1A**) when compared to Sham Vehicle. Meanwhile, smooth muscle-dependent aortic relaxation induced by sodium nitroprusside (SNP), a NO donor was seemingly unaffected by CS exposure, albeit a 20% reduction in maximal response (i.e. R_{max} at 10⁻⁵ M) was detected (**Figure 1B**). These findings suggest impairment of endothelial-dependent vasodilation by CS exposure. In line with this, our immunostaining detected a 50% reduction in vascular eNOS expression (**Figure 1C**), together with a concomitant 3-fold increase in 3-NT (**Figure 2A**) by CS exposure, suggesting a reduced bioavailability of endothelial NO and the presence of vascular oxidative stress. In line with this, increased adhesion of platelets to the endothelium and their activation were observed, marked by the increased fluorescence signal of CD41 (**Figure 2B**) and CD62p (**Figure 2C**), respectively, suggesting vascular injury. Apocynin treatment improved both the acetylcholine-stimulated and SNP-induced vasodilatory response (**Figure 1A-B**), which were associated with preserved eNOS expression (**Figure 1C**) and lessened vascular oxidative stress (**Figure 2A**), thus reducing the adhesion and activation of platelets at the vascular endothelium (**Figure 2B-C**). Meanwhile, no significant effects were found on the heart weight following CS exposure and/or apocynin treatment (**Figure S1L**), suggesting the cardiovascular defects in our model are mainly located in the vasculature.

Apocynin treatment attenuated the suppressive effect of CS exposure on body weight gain and lymphocytosis.

Consistent with the suppressive effects on weight gain observed in humans (Chan et al., 2019), chronic CS exposure markedly reduced body weight gain in mice (**Figure 3A**), which was attributed to ~12% loss in overall lean mass (**Figure 3B**) and ~50% loss in overall fat mass (**Figure 3C**). Despite the lack of effects on fat mass, apocynin treatment attenuated the suppressive effect of CS exposure on lean mass (**Figure 3B-C**), suggesting apocynin treatment assisted in the preservation of lean mass against CS exposure, consistent with the improved body weight observed in the apocynin-treated animals at the end of the study (**Figure 3A**). In contrast to the BALF data, CS exposure specifically increased (2-fold) blood lymphocyte counts (**Figure 3D-G**), marking the systemic lymphocytosis and chronic inflammation .

Consistent with its renowned antioxidant and -inflammatory effects , apocynin treatment attenuated CS-induced lymphocytosis.

Long term apocynin treatment reduced lung function decline, airway fibrosis and inflammation caused by CS exposure.

The promising benefits observed in the 8-week protocol have prompted us to investigate whether apocynin administration may alter the development of COPD. CS exposure for 24 weeks resulted in lung function decline and emphysema marked by a left-shift in the PV-loop curve (**Figure 4A**) as well as increases in static compliance (**Figure 4B**), PV loop area (**Figure 4C**), IC (**Figure 4D**) and FVC (**Figure 4E**), suggesting hyperinflation of the lungs. The increase of PV loop area and IC were significantly reduced by apocynin treatment. Apocynin treatment also inhibited the thickening of the small airway epithelium and excessive collagen deposition caused by CS exposure (**Figure 5A**), which is associated with airway stiffening (Liu et al., 2021). Despite the renowned effect of habitual smoking on airway mucus hypersecretion in humans (Allinson et al.), no mucus congestions were found in the airways of CS-exposed mice (**Figure S2**), suggesting mucus hypersecretion is unlikely to be driven by CS exposure *per se*. Compared to the 8-week protocol, apocynin treatment had a more noticeable benefit on CS-induced airway inflammation, evidenced by a reduction in total number of cells (by 21%), macrophages (by 33%), neutrophil (by 20%) and lymphocytes (by 47%) counts in the BALF (**Figure 5B-E**). Accordingly, the CS-induced expression of pro-inflammatory mediators (*Tnfa*, *Il6* and *Mmp12*; **Figure 5F-H**) and *Cybb* (**Figure 5I**) were significantly reduced by apocynin treatment.

Long term apocynin treatment preserved vascular endothelial function against CS exposure.

Similar to that of the 8-week protocol, mice exposed to CS for 24 weeks displayed ~67% reduction in weight gain compared to the Sham group (**Figure 6A**), attributing to ~13% and ~36% loss in lean and fat mass, respectively (**Figure 6B-C**), which were unaltered by apocynin treatment. Unlike that of the 8-week protocol, 24 weeks of CS exposure resulted in a 2-fold increase in blood granulocytes count which was prevented by apocynin treatment (**Figure 6D-G**). Apocynin treatment also prevented the CS-induced increase in haematocrit (**Figure 6H**), which is an indicator of chronic hypoxia (Kent et al., 2011). Similar to that of the 8-week protocol, CS exposure caused a marked impairment in the acetylcholine-mediated vasodilation, leaving the SNP-stimulated vasodilation unaltered (**Figure 6I**). In agreement with this, eNOS expression (**Figure 7A**) was diminished by 24 weeks of CS exposure, which may be attributed to an increased oxidative modifications of the aorta (**Figure 7B**). This was accompanied by increased platelet adhesion (CD41) and activation (CD62p) at the vascular endothelium (**Figure 7C-D**). Apocynin treatment preserved maximal acetylcholine-mediated vasodilation by ~60% (R_{max} ; **Figure 6I**) in CS-exposed mice. In line with this, the availability of eNOS, oxidative modifications of the aorta, and platelet adhesion/activation (**Figure 7A-D**) were normalised, suggesting the inhibitory effects of apocynin treatment may offer long-term protection against vascular oxidative stress and endothelial dysfunction.

Discussion

The present study sought to understand the benefits of apocynin treatment on CS-induced pulmonary and vascular pathologies. CS exposure caused significant airway inflammation, vascular dysfunction, and platelet reactivity. By limiting oxidative stress, apocynin treatment attenuated airway inflammation, and prevented the onset of both vascular dysfunction and platelet reactivity by CS exposure. We found that long-term apocynin treatment had marked benefits on airway inflammation and attenuated the progression of COPD, with reduced pulmonary hyperinflation and airway fibrosis arising from chronic CS exposure. These findings support modulating oxidative stress as viable strategies for the management of COPD.

Chronic inflammation is the most important feature of CS exposure and the strongest driver of pulmonary (Hikichi et al., 2019) and systemic pathologies (Brassington et al., 2019; Chan et al., 2019) in COPD. The chronic inflammatory process in COPD involves both innate and adaptive immunity and is most pronounced in the bronchial walls of the small airways (King, 2015). Chronic inflammation of the airway leads to the accumulation of inflammatory mucus exudates in the lumen and increased tissue volume of the bronchial wall (Cosio et al., 2009). The increased tissue volume of the bronchial wall is a result of infiltration by both innate (macrophages and neutrophils) and adaptive immune cells (lymphocytes), leading to the airflow obstruction/chronic bronchitis seen in COPD (Barnes, 2016). Meanwhile the development of emphysema appears to be closely linked to the infiltration of macrophages and neutrophils into the lung parenchyma (Barnes, 2020). CS exposure increases their recruitment and activation in the respiratory tract, leading to the production of various proinflammatory mediators, including cytokines/chemokines (TNF- α , IL-6 and CCL2), ROS (superoxide and NO), and proteases (MMP9 and 12) (Stampfli et al., 2009) that drives the development of emphysema (Barnes, 2016). The production of these proinflammatory mediators is triggered by the activation of Toll like receptors (TLRs) and lymphocyte antigen receptors, resulting in the activation of the signal transducers and activators of transcription (STATs)/ NF- κ B intracellular signaling pathways (Vlahos et al., 2015; Vlahos et al., 2018). In line with this, our preclinical model recapitulated the chronic airway inflammation, immune cell infiltration, and the consequential decline in lung function and emphysema manifestation at the 6-month time point. Strikingly, CS exposure was associated with a distinct increase in blood lymphocyte count (at 2-month) and neutrophil count (at 6-month), suggesting the driving force of systemic inflammation in COPD is unlikely to be mutually exclusive and may involve the dynamic action of inflammatory cells from both innate and adaptive immunity. On this note, it is understood that the inflammatory process in COPD has marked heterogeneity (King, 2015) depending on several extrinsic factors such as smoke history, age, lifestyle and current medications (Alabi et al., 2021). This is further complicated by acute exacerbations which may lead to several different endotypes driven by neutrophils, eosinophils, dendritic cells and mast cells (Barnes, 2019). Our results highlight that chronic CS exposure *per se* may produce distinct systemic inflammatory profile independent of exacerbations or the influence of the aforementioned extrinsic factors.

It is well-established that COPD increases the risk of CVD by two to four-fold (Shaw et al., 2014), which may be attributed to systemic inflammation (Thomsen et al., 2012). Clinically, systemic inflammation in COPD is often identified by the increase of several biomarkers in the circulation, such as C-reactive protein (CRP), IL-6, IL-8, TNF- α , fibrinogen and leukocyte (Cardoso et al., 2021). However, it is noteworthy that systemic inflammation is not a stable

feature in all patients with COPD, with considerable variations from time to time even within the same individual (Cardoso et al., 2021). In 8,656 patients with COPD from two large Danish population, Thomsen *et al* (Thomsen et al., 2012) observed a greater risk of CVD-related hospitalization or death compared to the non-COPD counterparts, despite only 10% of the COPD patients displaying elevated levels of all three of the biomarkers measured (CRP, fibrinogen, and leukocyte), suggesting the predictive power of these biomarkers on CVD risk in COPD, even when presented *in silos*. In line with the increased CVD risk, mice exposed to CS displayed impaired vasodilation. Impaired vasodilation can be a result of either the endothelium failing to send vasodilatory signals to the smooth muscle due to the loss of endothelial layer integrity (endothelial-dependent) or the smooth muscle cells not responding to endothelial signaling and dilate (endothelial-independent). Our result suggested that CS exposure specifically dampens eNOS action and endothelium-dependent vasodilation, while the vascular smooth muscle dilatory response was unaffected, regardless of CS exposure duration. This is somewhat surprising, as nicotine has been shown to diminish endothelium-independent vasodilation via the production of superoxide anion, which impairs the action of ATP-sensitive K⁺ channels on voltage gated Ca²⁺ channels (Mayhan et al., 2002). Moreover, CS-derived nicotine has been shown to enhance vasoconstrictive response of the vascular smooth muscle to phenylephrine (Olfert et al., 2018; Sarabi et al., 2000), suggesting its amplifying effect on α 1-adrenergic receptor activation. However, studies in mice (Brassington et al., 2021; Olfert et al., 2018) and smokers (Sarabi et al., 2000) have found that SNP-induced vasodilation is generally preserved. The reason for this discrepancy is unclear, though recent work by Oakes et al (Oakes et al., 2020) demonstrated that chronic nicotine exposure also increases the body's tolerance to the hypertensive effects of nicotine, which may explain the seemingly unaltered SNP-induced vasodilation in our study.

In addition to vasodilation impairment, increased platelet reactivity may also arise from habitual smoking (Brassington et al., 2019). Increased platelet reactivity promotes dysregulated platelet aggregation which is associated with increased risk of myocardial infarction, terminal occlusive thrombotic events, and sudden death in patients with COPD (Brassington et al., 2019). Firstly, CS exposure has been shown to directly cause platelet activation and their aggregation via the activation of the Cyclooxygenase-1 pathway (Loke et al., 2014). Secondly, the spill-over of pro-inflammatory mediators from the COPD lungs into the vasculature may cause the adhesion of activated platelets to the arterial wall and collagen fibres, via the up-regulation of CD41, p-selectin (CD62p) and von Willibrand factor (Jennings, 2009). Thirdly, endothelial dysfunction constitutes vascular injury which may stimulate platelets aggregation and adhesion to the endothelium, releasing platelet-derived growth factors to promote formation of thrombo-embolism consisting of platelets, endothelial cells, monocytes and erythrocytes at the site of the injury (Hamilos et al., 2018). Of interest, both platelet aggregation (Pamukcu et al., 2011) and platelet-derived Cyclooxygenase-1 expression (Loke et al., 2014) were markedly elevated in habitual smokers, independent of acute smoking. This suggests platelet activation and aggregation is likely to be a consequence of long-term repeated exposure to CS.

In line with its antioxidant and anti-inflammatory properties (Petronio et al., 2013), both CS-induced airway and systemic inflammation were effectively reduced by apocynin treatment, particularly with long-term administration. Although lung function decline and emphysema remained evidenced, apocynin treatment lessened hyperinflation of the lungs, which was associated with a marked reduction in epithelium thickening and fibrosis of the small airway.

Hyperinflation has been shown to reduce gas exchange capacity which results in persisting hypoxia, eliciting adverse pulmonary vascular remodelling and pulmonary hypertension (Dunham-Snary et al., 2017). In line with this, we detected an increase in haematocrit percentage, suggesting the presence of hypoxemia following long-term CS exposure. Meanwhile, hyperinflation is caused by air trapping which is strongly linked to increase intensity of dyspnoea (Barnes, 2019). Together, both hypoxemia and dyspnoea form a vicious spiral of activity avoidance, physical deconditioning, and reduced quality of life, thereby accelerating the development of extra-pulmonary comorbidities such as CVD (Rabe et al., 2018). Clinically, long-acting bronchodilator treatment has been shown to reduce hyperinflation in COPD (Di Marco et al., 2018). Our study demonstrated that apocynin treatment reduced both of these CS-induced impairments, suggesting apocynin may be used in conjunction with long-acting bronchodilator to improve gas-exchange and reduce exertional dyspnoea in COPD. This in turn would increase a patient's ability to exercise and their likelihood to benefit from pulmonary rehabilitation. In terms of vascular function, apocynin treatment offered complete preservation of eNOS expression and endothelium-dependent vasodilation against continuous CS exposure. This finding supports the notion that limiting oxidative stress and systemic inflammation as a viable treatment strategy for pulmonary and systemic comorbidities in COPD. More importantly, our study also raises the concept that oxidative stress should be incorporated as a part of the new treatable trait approach for COPD (Cardoso et al., 2021; Duszyk et al., 2021), given oxidative stress and inflammation are known to perpetuate each other (Barnes, 2022). Therefore, treatments that disrupt/stop this vicious cycle should benefit people with COPD, much similar to that of apocynin treatment in our preclinical COPD model.

In summary, the present study demonstrated that habitual CS exposure is linked to vascular dysfunction and increased platelet reactivity *in vivo*, which may be alleviated by the inhibition of oxidative stress. Both airway and systemic inflammation are recognised treatable traits of COPD, however, oxidative stress is surprisingly yet to be included. Clinically, oxidative stress may be measured by a number of biomarkers present in exhaled breath such as 8-isoprostane (Montuschi et al., 2000), H₂O₂ (Nowak et al., 2001), nitric oxide metabolites (NO²⁻/NO³⁻) (Balint et al., 2001), and/or those from blood like malondialdehyde (Lykkesfeldt et al., 2004), thiobarbituric acid reactive substances (Del Rio et al., 2005), carbonyl derivatives (Zinellu et al., 2016), and ferric ion levels (Zinellu et al., 2016). Future studies should examine the clinical feasibility and benefit of treating oxidative stress on key health outcomes, including 6-minute walk distance, spirometry and health-related quality of life score.

References

Adeloye D, Chua S, Lee C, Basquill C, Papana A, Theodoratou E, *et al.* (2015). Global and regional estimates of COPD prevalence: Systematic review and meta-analysis. *J Glob Health* 5: 020415.

Alabi FO, Alkhateeb HA, DeBarros KM, Barletti Benel PS, Sanchez-Martinez RL, Zeper ML, *et al.* (2021). The Heterogeneity of COPD Patients in a Community-Based Practice and the Inadequacy of the Global Initiative for Chronic Obstructive Lung Disease Criteria: A Real-World Experience. *Chronic Obstr Pulm Dis* 8: 396-407.

Alexander SPH, Roberts RE, Broughton BRS, Sobey CG, George CH, Stanford SC, *et al.* (2018). Goals and practicalities of immunoblotting and immunohistochemistry: A guide for submission to the British Journal of Pharmacology. *Br J Pharmacol* 175: 407-411.

Allinson JA-O, Hardy RA-O, Donaldson GA-O, Shaheen SO, Kuh DA-O, & Wedzicha JA-O (2016). The Presence of Chronic Mucus Hypersecretion across Adult Life in Relation to Chronic Obstructive Pulmonary Disease Development.

Balbirsingh V, Mohammed AS, Turner AM, & Newnham M (2022). Cardiovascular disease in chronic obstructive pulmonary disease: a narrative review. *Thorax*.

Balint B, Donnelly LE, Hanazawa T, Kharitonov SA, & Barnes PJ (2001). Increased nitric oxide metabolites in exhaled breath condensate after exposure to tobacco smoke. *Thorax* 56: 456-461.

Barnes PJ (2016). Inflammatory mechanisms in patients with chronic obstructive pulmonary disease. *J Allergy Clin Immunol* 138: 16-27.

Barnes PJ (2019). Inflammatory endotypes in COPD. *Allergy* 74: 1249-1256.

Barnes PJ (2020). Oxidative stress-based therapeutics in COPD. *Redox Biol* 33: 101544.

Barnes PJ (2022). Oxidative Stress in Chronic Obstructive Pulmonary Disease. *Antioxidants (Basel)* 11.

Brassington K, Chan SMH, De Luca SN, Dobric A, Almerdasi SA, Mou K, *et al.* (2022). Ebselen abolishes vascular dysfunction in influenza A virus-induced exacerbations of cigarette smoke-induced lung inflammation in mice. *Clin Sci (Lond)* 136: 537-555.

Brassington K, Chan SMH, Seow HJ, Dobric A, Bozinovski S, Selemidis S, *et al.* (2021). Ebselen reduces cigarette smoke-induced endothelial dysfunction in mice. *Br J Pharmacol* 178: 1805-1818.

Brassington K, Selemidis S, Bozinovski S, & Vlahos R (2019). New frontiers in the treatment of comorbid cardiovascular disease in chronic obstructive pulmonary disease. *Clin Sci (Lond)* 133: 885-904.

Cardoso J, Ferreira AJ, Guimaraes M, Oliveira AS, Simao P, & Sucena M (2021). Treatable Traits in COPD - A Proposed Approach. *Int J Chron Obstruct Pulmon Dis* 16: 3167-3182.

Chan SMH, Bernardo I, Mastronardo C, Mou K, De Luca SN, Seow HJ, *et al.* (2021). Apocynin prevents cigarette smoking-induced loss of skeletal muscle mass and function in mice by preserving proteostatic signalling. *Br J Pharmacol* 178: 3049-3066.

Chan SMH, Cerni C, Passey S, Seow HJ, Bernardo I, van der Poel C, *et al.* (2020). Cigarette Smoking Exacerbates Skeletal Muscle Injury without Compromising Its Regenerative Capacity. *Am J Respir Cell Mol Biol* 62: 217-230.

Chan SMH, Selemidis S, Bozinovski S, & Vlahos R (2019). Pathobiological mechanisms underlying metabolic syndrome (MetS) in chronic obstructive pulmonary disease (COPD): clinical significance and therapeutic strategies. *Pharmacol Ther* 198: 160-188.

Cosio MG, Saetta M, & Agusti A (2009). Immunologic aspects of chronic obstructive pulmonary disease. *N Engl J Med* 360: 2445-2454.

Curtis MJ, Alexander S, Cirino G, Docherty JR, George CH, Giembycz MA, *et al.* (2018). Experimental design and analysis and their reporting II: updated and simplified guidance for authors and peer reviewers. *Br J Pharmacol* 175: 987-993.

Del Rio D, Stewart AJ, & Pellegrini N (2005). A review of recent studies on malondialdehyde as toxic molecule and biological marker of oxidative stress. *Nutr Metab Cardiovasc Dis* 15: 316-328.

Di Marco F, Sotgiu G, Santus P, O'Donnell DE, Beeh KM, Dore S, *et al.* (2018). Correction to: Long-acting bronchodilators improve exercise capacity in COPD patients: a systematic review and meta-analysis. *Respir Res* 19: 70.

Dobric A, De Luca SN, Seow HJ, Wang H, Brassington K, Chan SMH, *et al.* (2022). Cigarette Smoke Exposure Induces Neurocognitive Impairments and Neuropathological Changes in the Hippocampus. *Front Mol Neurosci* 15: 893083.

Dunham-Snary KJ, Wu D, Sykes EA, Thakrar A, Parlow LRG, Mewburn JD, *et al.* (2017). Hypoxic Pulmonary Vasoconstriction: From Molecular Mechanisms to Medicine. *Chest* 151: 181-192.

Duszyk K, McLoughlin RF, Gibson PG, & McDonald VM (2021). The use of treatable traits to address COPD complexity and heterogeneity and to inform the care. *Breathe (Sheff)* 17: 210118.

Hamilos M, Petousis S, & Parthenakis F (2018). Interaction between platelets and endothelium: from pathophysiology to new therapeutic options. *Cardiovasc Diagn Ther* 8: 568-580.

Hikichi M, Mizumura K, Maruoka S, & Gon Y (2019). Pathogenesis of chronic obstructive pulmonary disease (COPD) induced by cigarette smoke. *J Thorac Dis* 11: S2129-S2140.

Hlapić I, Somborac-Bacura A, Popović-Grle S, Vukić Dugac A, Rogić D, Rako I, *et al.* (2020). Platelet indices in stable chronic obstructive pulmonary disease - association with inflammatory markers, comorbidities and therapy. *Biochem Med (Zagreb)* 30: 010701.

Jennings LK (2009). Role of platelets in atherothrombosis. *Am J Cardiol* 103: 4A-10A.

Kent BD, Mitchell PD, & McNicholas WT (2011). Hypoxemia in patients with COPD: cause, effects, and disease progression. *Int J Chron Obstruct Pulmon Dis* 6: 199-208.

King PT (2015). Inflammation in chronic obstructive pulmonary disease and its role in cardiovascular disease and lung cancer. *Clin Transl Med* 4: 68.

Liu L, Stephens B, Bergman M, May A, & Chiang T (2021). Role of Collagen in Airway Mechanics. *Bioengineering (Basel)* 8.

Loke WM, Sing KL, Lee CY, Chong WL, Chew SE, Huang H, *et al.* (2014). Cyclooxygenase-1 mediated platelet reactivity in young male smokers. *Clin Appl Thromb Hemost* 20: 371-377.

Lykkesfeldt J, Viscovich M, & Poulsen HE (2004). Plasma malondialdehyde is induced by smoking: a study with balanced antioxidant profiles. *Br J Nutr* 92: 203-206.

Mayhan WG, & Sharpe GM (2002). Acute and chronic treatment with nicotine impairs reactivity of arterioles in response to activation of potassium channels. *J Cardiovasc Pharmacol* 39: 695-703.

Montuschi P, Collins JV, Ciabattini G, Lazzeri N, Corradi M, Kharitonov SA, *et al.* (2000). Exhaled 8-isoprostane as an in vivo biomarker of lung oxidative stress in patients with COPD and healthy smokers. *Am J Respir Crit Care Med* 162: 1175-1177.

Nowak D, Kalucka S, Bialasiewicz P, & Krol M (2001). Exhalation of H₂O₂ and thiobarbituric acid reactive substances (TBARs) by healthy subjects. *Free Radic Biol Med* 30: 178-186.

Oakes JM, Xu J, Morris TM, Fried ND, Pearson CS, Lobell TD, *et al.* (2020). Effects of Chronic Nicotine Inhalation on Systemic and Pulmonary Blood Pressure and Right Ventricular Remodeling in Mice. *Hypertension* 75: 1305-1314.

Olfert IM, DeVallance E, Hoskinson H, Branyan KW, Clayton S, Pitzer CR, *et al.* (2018). Chronic exposure to electronic cigarettes results in impaired cardiovascular function in mice. *J Appl Physiol* (1985) 124: 573-582.

Olukman M, Orhan CE, Celenk FG, & Ulker S (2010). Apocynin restores endothelial dysfunction in streptozotocin diabetic rats through regulation of nitric oxide synthase and NADPH oxidase expressions. *J Diabetes Complications* 24: 415-423.

Oostwoud LC, Gunasinghe P, Seow HJ, Ye JM, Selemidis S, Bozinovski S, *et al.* (2016). Apocynin and ebselen reduce influenza A virus-induced lung inflammation in cigarette smoke-exposed mice. *Sci Rep* 6: 20983.

Pamukcu B, Oflaz H, Onur I, Cimen A, & Nisanci Y (2011). Effect of cigarette smoking on platelet aggregation. *Clin Appl Thromb Hemost* 17: E175-180.

Petronio MS, Zeraik ML, Fonseca LM, & Ximenes VF (2013). Apocynin: chemical and biophysical properties of a NADPH oxidase inhibitor. *Molecules* 18: 2821-2839.

Rabe KF, Hurst JR, & Suissa S (2018). Cardiovascular disease and COPD: dangerous liaisons? *Eur Respir Rev* 27.

Safiri S, Carson-Chahhoud K, Noori M, Nejadghaderi SA, Sullman MJM, Ahmadian Heris J, *et al.* (2022). Burden of chronic obstructive pulmonary disease and its attributable risk factors in 204 countries and territories, 1990-2019: results from the Global Burden of Disease Study 2019. *BMJ* 378: e069679.

Sarabi M, & Lind L (2000). Short-term effects of smoking and nicotine chewing gum on endothelium-dependent vasodilation in young healthy habitual smokers. *J Cardiovasc Pharmacol* 35: 451-456.

Shaw JG, Vaughan A, Dent AG, O'Hare PE, Goh F, Bowman RV, *et al.* (2014). Biomarkers of progression of chronic obstructive pulmonary disease (COPD). *J Thorac Dis* 6: 1532-1547.

Sin DD, Wu L, & Man SF (2005). The relationship between reduced lung function and cardiovascular mortality: a population-based study and a systematic review of the literature. *Chest* 127: 1952-1959.

Stampfli MR, & Anderson GP (2009). How cigarette smoke skews immune responses to promote infection, lung disease and cancer. *Nat Rev Immunol* 9: 377-384.

Theodorakopoulou MP, Alexandrou ME, Bakaloudi DR, Pitsiou G, Stanopoulos I, Kontakiotis T, *et al.* (2021). Endothelial dysfunction in COPD: a systematic review and meta-analysis of studies using different functional assessment methods. *ERJ Open Res* 7.

Thomsen M, Dahl M, Lange P, Vestbo J, & Nordestgaard BG (2012). Inflammatory biomarkers and comorbidities in chronic obstructive pulmonary disease. *Am J Respir Crit Care Med* 186: 982-988.

Vlahos R, & Bozinovski S (2015). Preclinical murine models of Chronic Obstructive Pulmonary Disease. *Eur J Pharmacol* 759: 265-271.

Vlahos R, & Bozinovski S (2018). Modelling COPD co-morbidities in preclinical models. *Respirology* 23: 1094-1095.

Vlahos R, Stambas J, Bozinovski S, Broughton BR, Drummond GR, & Selemidis S (2011). Inhibition of Nox2 oxidase activity ameliorates influenza A virus-induced lung inflammation. *PLoS Pathog* 7: e1001271.

Wang H, Aloe C, McQualter J, Papanicolaou A, Vlahos R, Wilson N, *et al.* (2021). G-CSFR antagonism reduces mucosal injury and airways fibrosis in a virus-dependent model of severe asthma. *Br J Pharmacol* 178: 1869-1885.

Chronic obstructive pulmonary disease fact sheet. [Online] Available from [https://www.who.int/news-room/fact-sheets/detail/chronic-obstructive-pulmonary-disease-\(copd\)](https://www.who.int/news-room/fact-sheets/detail/chronic-obstructive-pulmonary-disease-(copd)). [Accessed: 11 November 2022].

Zinellu E, Zinellu A, Fois AG, Carru C, & Pirina P (2016). Circulating biomarkers of oxidative stress in chronic obstructive pulmonary disease: a systematic review. *Respir Res* 17: 150.

Figure legends

Figure 1. CS-induced vascular dysfunction and platelet activation were attenuated by apocynin treatment. Mice were exposed to cigarette smoke (CS) or room air (Sham) for 8 weeks with i.p. injection of apocynin ($5 \text{ mg}\cdot\text{kg}^{-1}\cdot\text{day}^{-1}$) or vehicle (saline). Cumulative concentration response curves and EC_{50} analysis to acetylcholine (A) or sodium nitroprusside (B) ($1\times 10^{-8}\text{M}$ to $1\times 10^{-5}\text{M}$) to examine endothelial-dependent and endothelial-independent vasodilation in mouse thoracic aorta, respectively. Representative immunofluorescence images of thoracic aorta section stained with endothelial nitric oxide synthase (eNOS; C) Data are expressed as mean + SEM (n= 8 mice per group) and analyzed by two-way ANOVA with multiple comparisons and Tukey post-hoc test. * $p<0.05$, ** $p<0.01$, *** $p<0.001$, **** $p<0.0001$ denotes differences between the compared groups.

Figure 2. CS-induced vascular oxidative stress and platelet aggregation were prevented by apocynin treatment. Mice were exposed to cigarette smoke (CS) or room air (Sham) for 8 weeks with i.p. injection of apocynin ($5 \text{ mg}\cdot\text{kg}^{-1}\cdot\text{day}^{-1}$) or vehicle (saline). Representative immunofluorescence images of thoracic aorta section stained with 3-nitrotyrosine (3-NT; A), platelet surface marker (CD41; B), or platelet activation marker (CD62p; C), with positive staining in green and nuclei in blue (DAPI). White arrows indicate positive stains, and the respective positive stains were quantified as described in methods. Data are expressed as mean + SEM (n= 8 mice per group) and analyzed by two-way ANOVA with multiple comparisons and Tukey post-hoc test. * $p<0.05$, ** $p<0.01$, *** $p<0.001$, **** $p<0.0001$ denotes differences between the compared groups.

Figure 3. CS-induced loss of lean mass and systemic lymphocytosis were prevented by apocynin treatment. Mice were exposed to cigarette smoke (CS) or room air (Sham) for 8 weeks with i.p. injection of apocynin ($5 \text{ mg}\cdot\text{kg}^{-1}\cdot\text{day}^{-1}$) or vehicle (saline). Change in body weight (A), alterations in body lean (B) and fat (C) mass. Hematology analysis of total white blood cells (D), mid-range cells (E), granulocytes (F) and lymphocytes (G). Data are expressed as mean + SEM (n= 8 mice per group) and analyzed by two-way ANOVA with multiple comparisons and Tukey post-hoc test. * $p<0.05$, ** $p<0.01$, *** $p<0.001$, **** $p<0.0001$ denotes differences between the compared groups.

Figure 4. The CS-induced lung hyperinflation was lessened by apocynin treatment. Mice were exposed to cigarette smoke (CS) or room air (Sham) for 8 weeks with i.p. injection of apocynin ($5 \text{ mg}\cdot\text{kg}^{-1}\cdot\text{day}^{-1}$) or vehicle (saline). Different respiratory parameters from the lung function assessment, including PV ratio (A), static compliance (B), PV loop area (C), IC (D) and FVC (E). Data are expressed as mean + SEM (n= 8 mice per group) and analyzed by two-way ANOVA with multiple comparisons and Tukey post-hoc test. * $p<0.05$, ** $p<0.01$, *** $p<0.001$, **** $p<0.0001$ denotes differences between the compared groups.

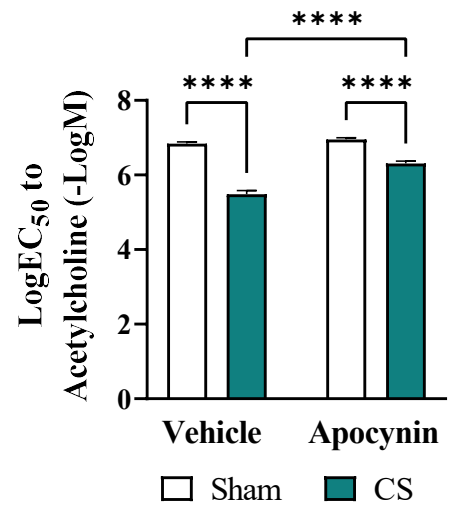
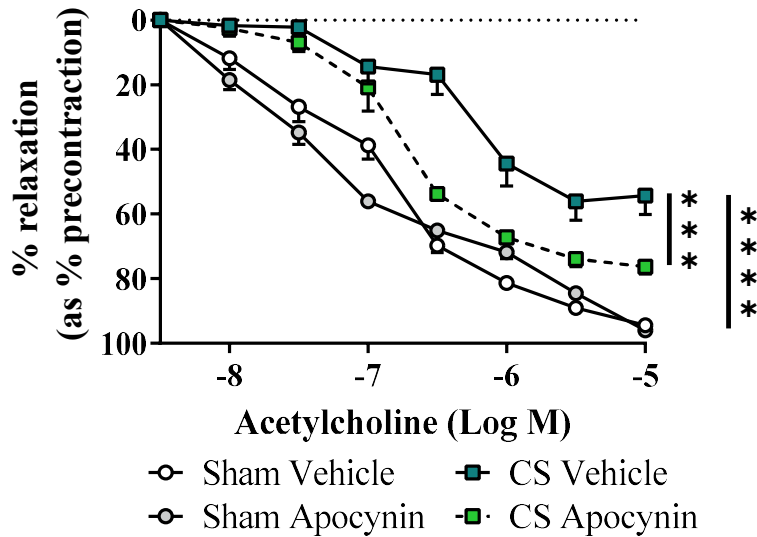
Figure 5. Long term CS-induced airway inflammation and fibrosis from were attenuated by apocynin treatment. Mice were exposed to cigarette smoke (CS) or room air (Sham) for 8 weeks with i.p. injection of apocynin ($5 \text{ mg}\cdot\text{kg}^{-1}\cdot\text{day}^{-1}$) or vehicle (saline). Representative maison trichome staining of cross-lung sections for collagen deposition surrounding smaller airways (A). Total number of cells (B), macrophage (C), neutrophils (D) and lymphocytes (E) in the BALF. Quantitative PCR was performed to assess the expression of *Tnfa* (F), *Il6* (G), *Mmp12* (H) and *Cybb* (I) in homogenized lung tissues. Data are expressed as mean + SEM (n= 8 mice per group) and analyzed by two-way ANOVA with multiple comparisons and Tukey post-hoc test. * $p<0.05$, ** $p<0.01$, *** $p<0.001$, **** $p<0.0001$ denotes differences between the compared groups.

Figure 6. Long term CS-induced systemic neutrophilia and vascular dysfunction were attenuated by apocynin treatment. Mice were exposed to cigarette smoke (CS) or room air (Sham) for 8 weeks with i.p. injection of apocynin ($5 \text{ mg} \cdot \text{kg}^{-1} \cdot \text{day}^{-1}$) or vehicle (saline). Change in body weight (A), alterations in body lean (B) and fat (C) mass. Hematology analysis of total white blood cell (D), monocytes (E), neutrophils (F), lymphocytes (G) and hematocrit (H). Cumulative concentration response curves and EC_{50} analysis to acetylcholine and sodium nitroprusside (I; $1 \times 10^{-8} \text{M}$ to $1 \times 10^{-5} \text{M}$) to examine endothelial-dependent and endothelial-independent vasodilation in mouse thoracic aorta, respectively. Data are expressed as mean + SEM ($n=8$ mice per group) and analyzed by two-way ANOVA with multiple comparisons and Tukey post-hoc test. * $p < 0.05$, ** $p < 0.01$, *** $p < 0.001$, **** $p < 0.0001$ denotes differences between the compared groups.

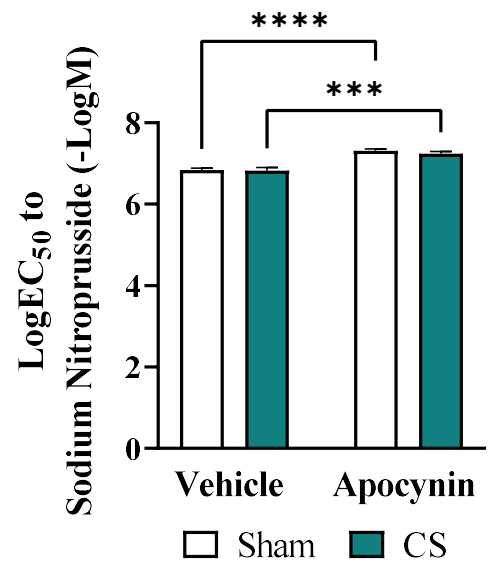
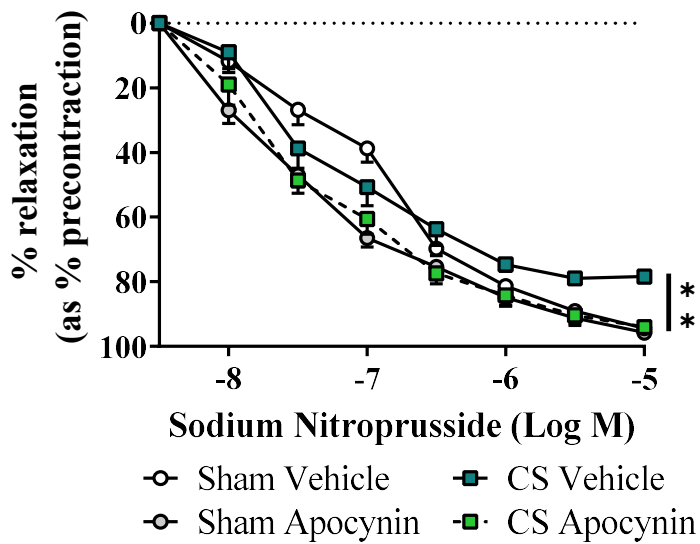
Figure 7. Long term CS-induced loss of eNOS, vascular oxidative stress and platelet activation were attenuated by apocynin treatment. Mice were exposed to cigarette smoke (CS) or room air (Sham) for 8 weeks with i.p. injection of apocynin ($5 \text{ mg} \cdot \text{kg}^{-1} \cdot \text{day}^{-1}$) or vehicle (saline). Representative immunofluorescence images of thoracic aorta section stained with eNOS (A), 3-NT (B), platelet surface CD41 (C), or platelet activation CD62p (D), with positive staining in green and nuclei in blue (DAPI). White arrows indicate positive stains, and the respective positive stains were quantified as described in methods. Data are expressed as mean + SEM ($n=8$ mice per group) and analyzed by two-way ANOVA with multiple comparisons and Tukey post-hoc test. ** $p < 0.01$, *** $p < 0.001$, **** $p < 0.0001$ denotes differences between the compared groups.

Figure 1: 8-week CS

A



B



C

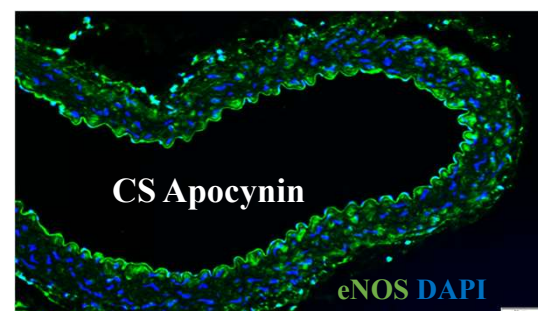
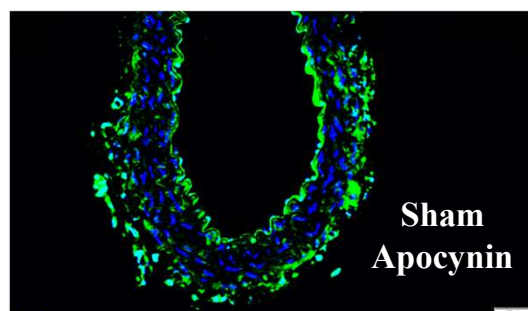
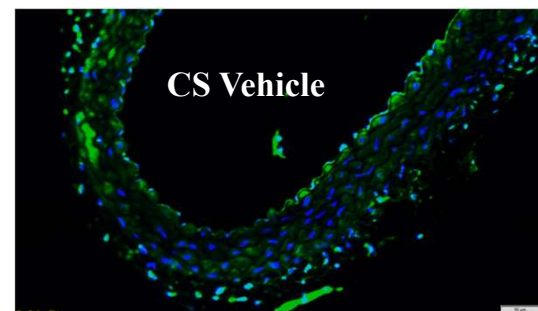
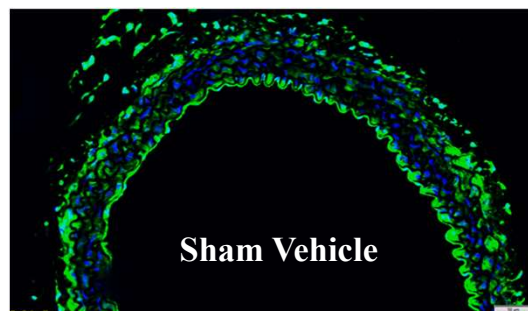
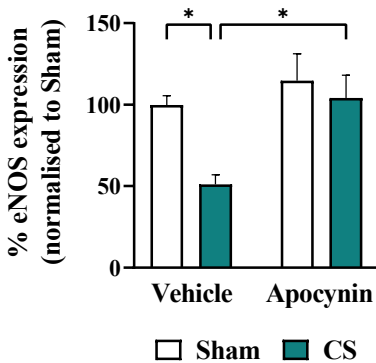
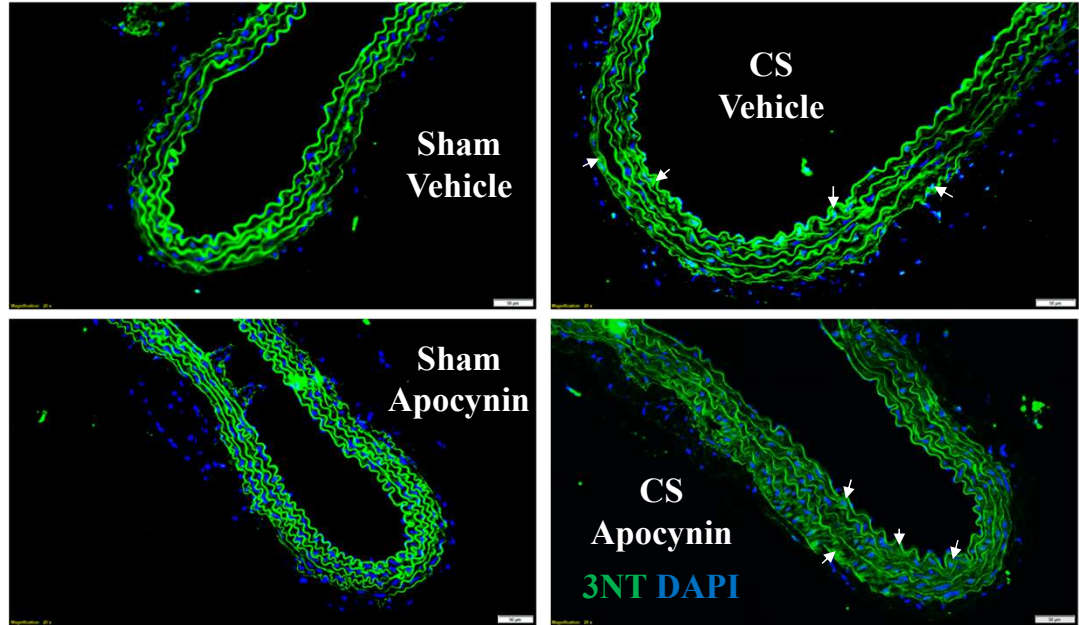
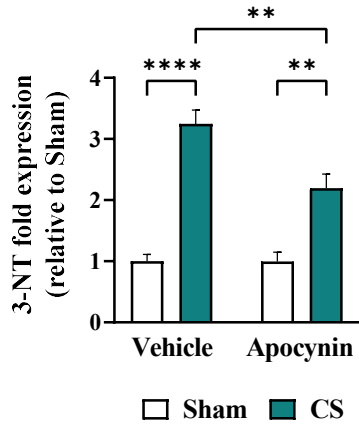
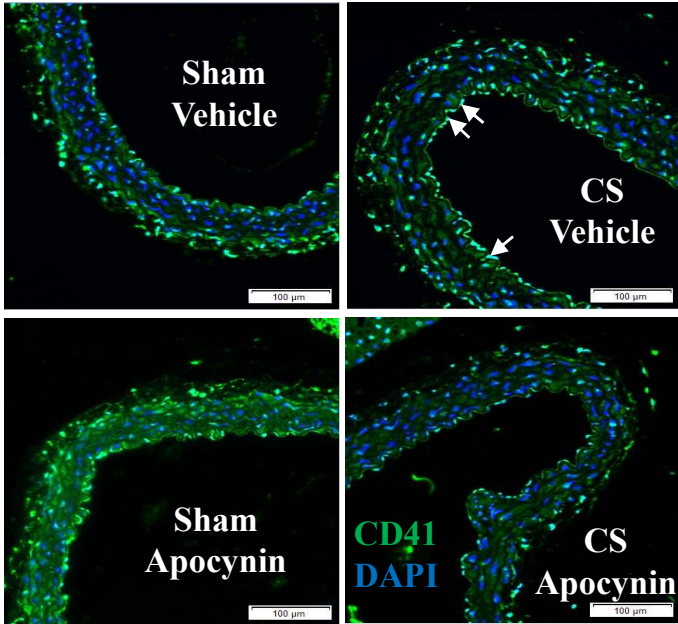
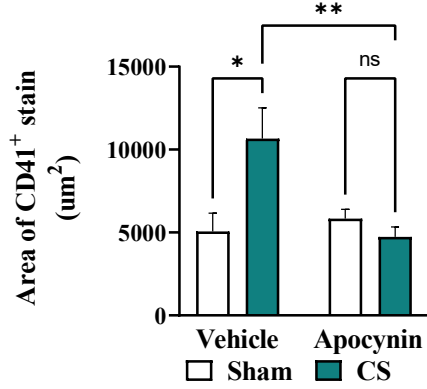


Figure 2: 8-week CS

A



B



C

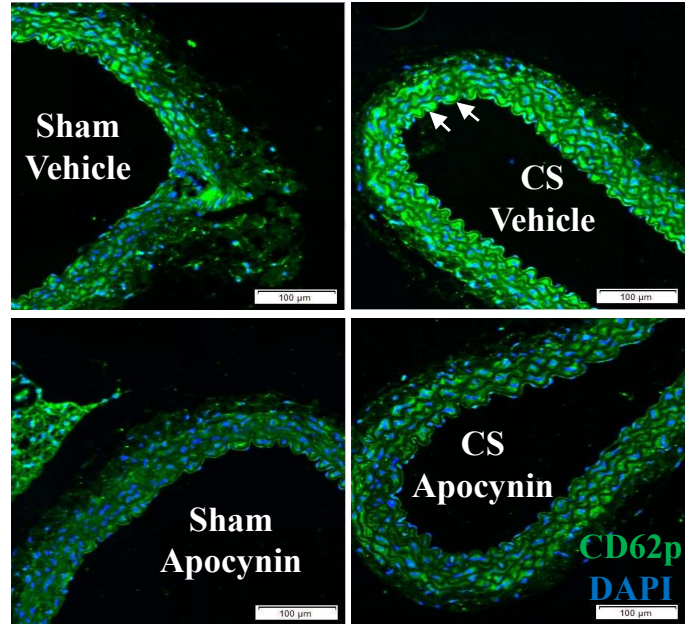
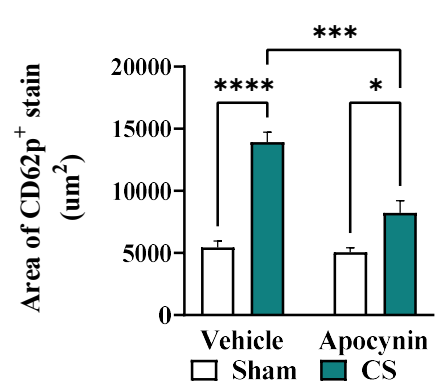


Figure 3: 8-week CS

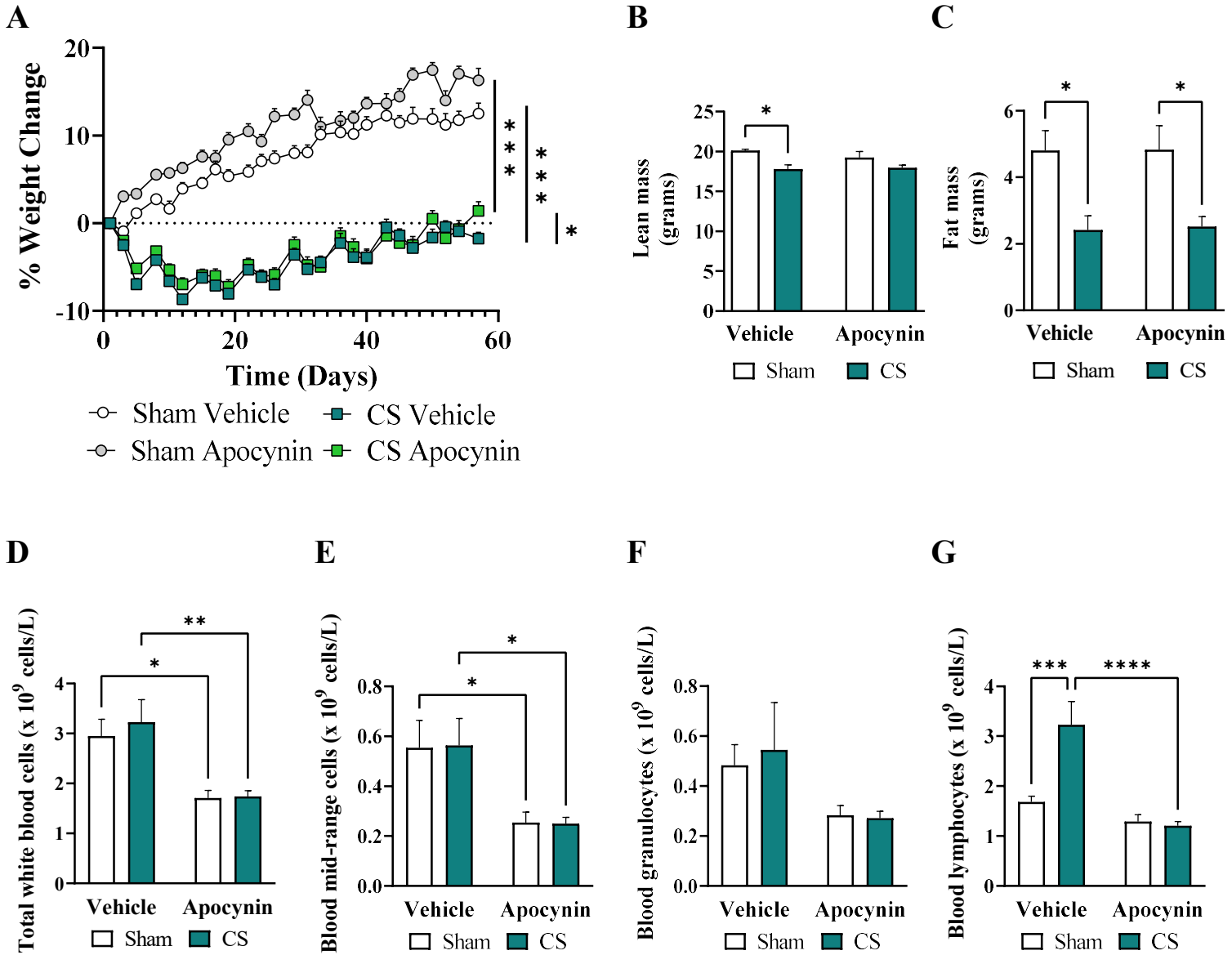


Figure 4: 24-week CS

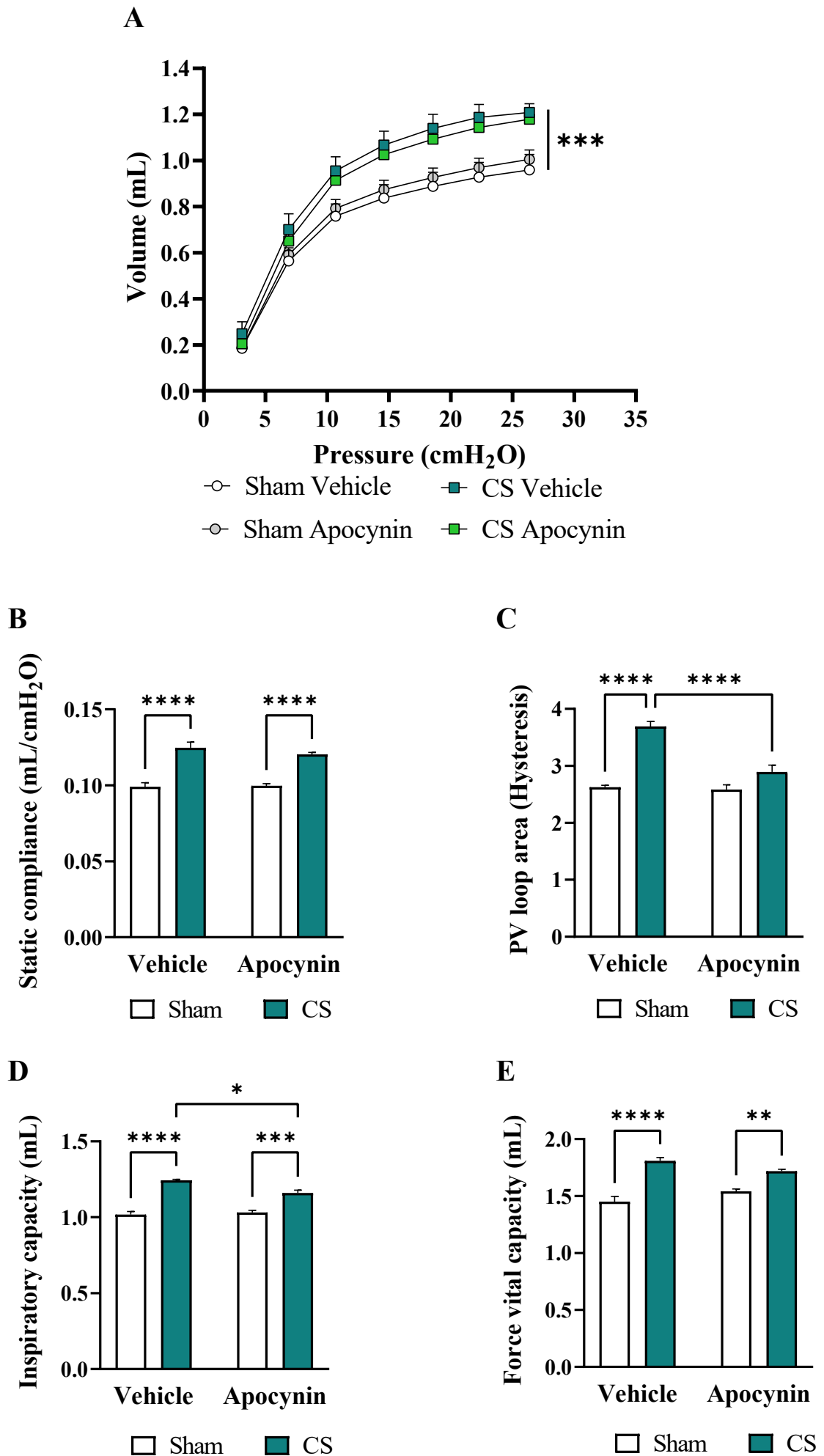
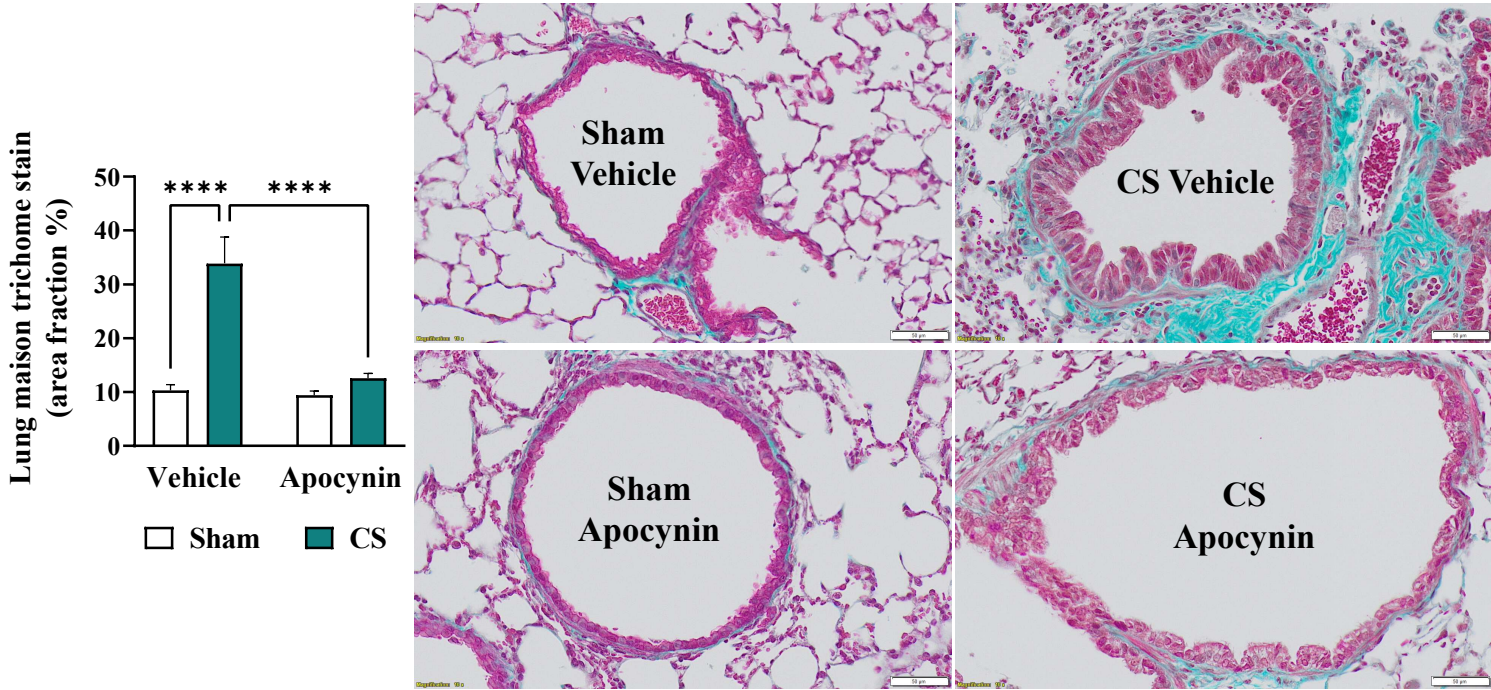
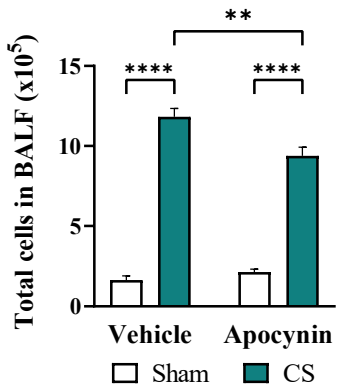


Figure 5: 24-week CS

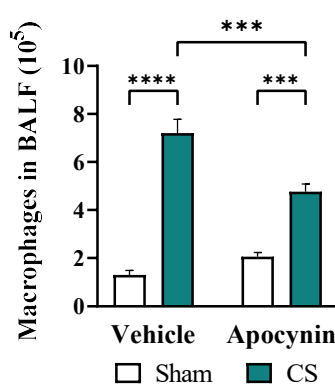
A



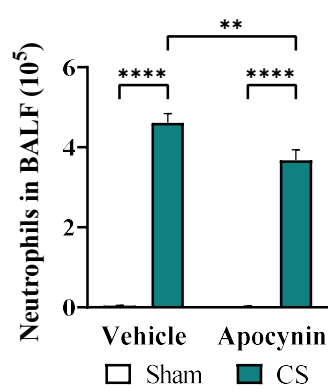
B



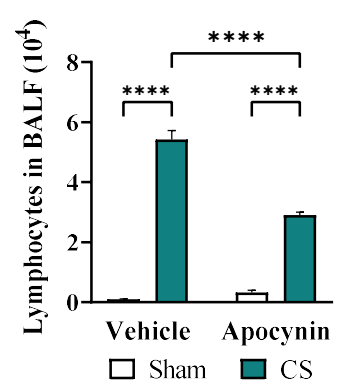
C



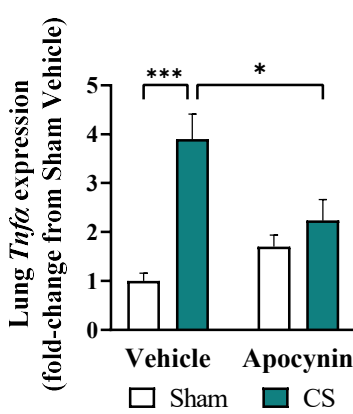
D



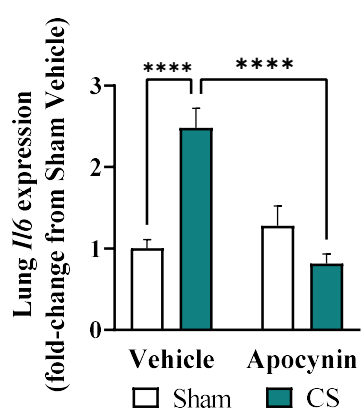
E



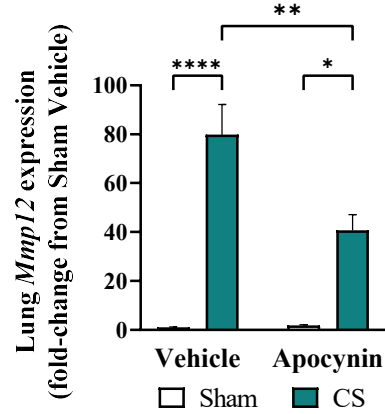
F



G



H



I

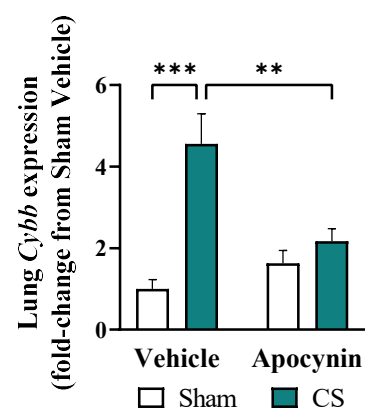


Figure 6: 24-week CS

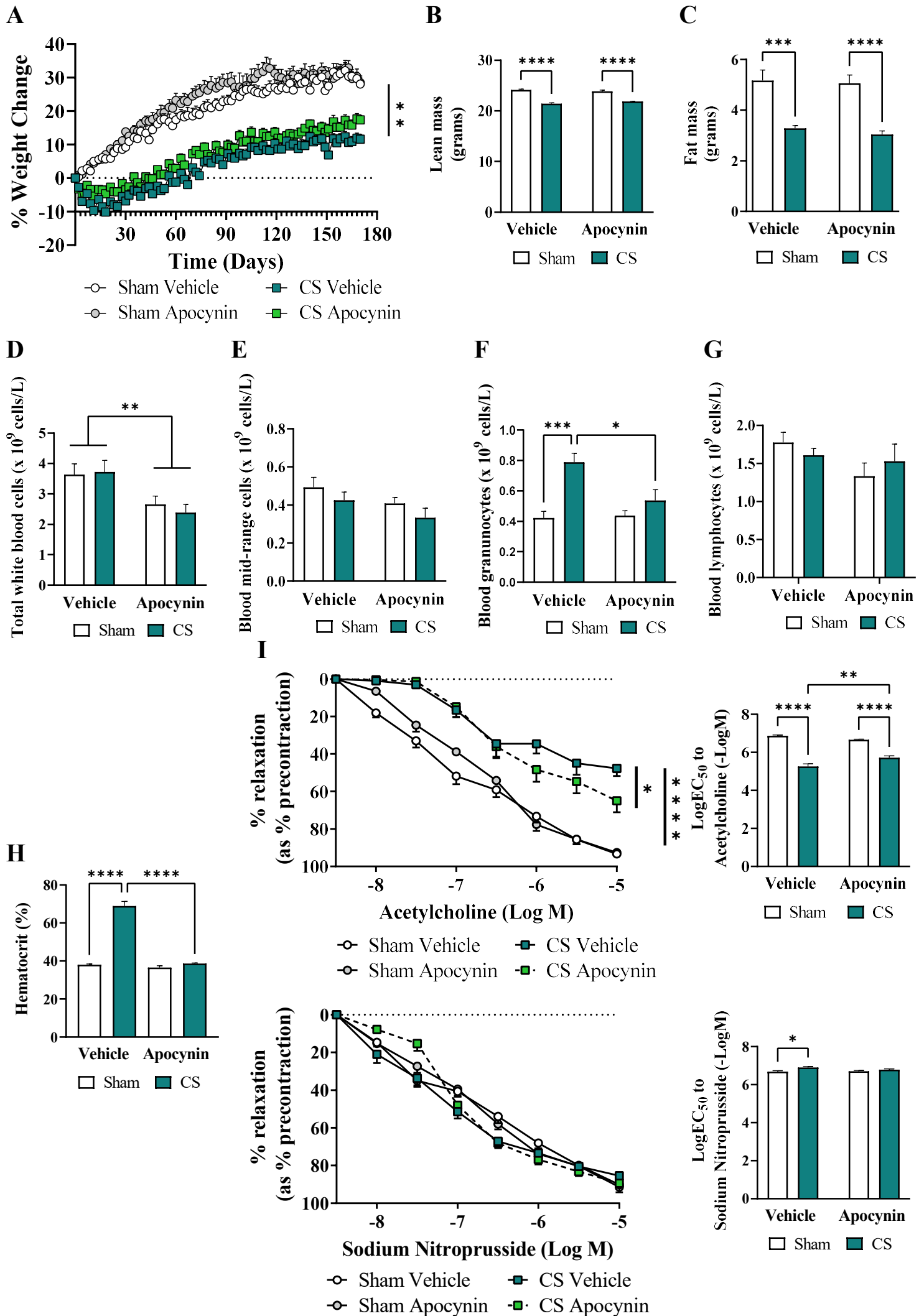


Figure 7: 24-week CS

